Optical study of Mn^{2+} ions environments in fluorochlorozirconate and fluorobromozirconate glasses

1998 J. Phys.: Condens. Matter 10 9343

(http://iopscience.iop.org/0953-8984/10/41/016)

J. Phys.: Condens. Matter **10** (1998) 9343–9358. Printed in the UK PII: S0953-8984(98)93163-0

Optical study of Mn^{2+} ions environments in fluorochlorozirconate and fluorobromozirconate glasses

M A Buñuel, R Alcalá and R Cases†

Instituto de Ciencia de Materiales de Aragon, Universidad de Zaragoza—CSIC, Facultad de Ciencias, Plza S Francisco s/n, 50009 Zaragoza, Spain

Received 7 April 1998, in final form 6 July 1998

Abstract. Some manganese doped fluorozirconate, fluorochloro- and fluorobromozirconate glasses have been prepared following and improving some standard methods. Electron probe microanalysis has been carried out to obtain the actual composition of the samples. The optical properties of Mn^{2+} ions, including steady state excitation and emission, and luminescence decay have been studied. Values of the crystal field and Racah parameters have been estimated from the excitation data. The results have been interpreted in terms of the progressive substitution of the fluorine ions in the first coordination shell of Mn^{2+} by chlorine or bromine ions. A concentration of about 6 at.% of chlorines or bromines with respect to the total number of halide ions is enough to have most of the Mn^{2+} ions coordinated to only chlorines or bromines.

1. Introduction

Heavy metal fluoride glasses (HMFG) have received great attention because of their applications as active optical materials [1, 2]. In order to improve their optical properties, some attempts to prepare heavy metal chloride or bromide glasses have been made. Unfortunately these glasses show low chemical stability and a great tendency to devitrification. Trying to obtain high stability and good optical properties, mixed glasses have been prepared in which small amounts of fluoride compounds are replaced by chlorides or bromides [3]. This substitution could be particularly interesting in the case of materials doped with rare earth ions. If fluorines could be replaced by heavier ions in the environment of the rare earth, the local phonon frequencies would decrease along with the multiphonon non-radiative deexcitation probabilities, resulting in an enhancement of the emission quantum yield. In order to study the arrangement of the chloride ions around the impurities, x-ray and infrared (IR) absorption, Raman spectroscopy and molecular dynamic simulation techniques have been applied to fluorochlorozirconate glasses [4–6]. The results indicate that the local structure in the vicinity of the Zr^{4+} ion is hardly affected and the chloride ions occupy non-bridging sites. Besides, some studies of 'up-conversion' in Er^{3+} doped fluorochlorozirconate glasses indicate the substitution of fluorine ions by chlorine ones as first neighbours of Er^{3+} [7, 8] which is in agreement with the structural studies indicated above.

3d ions are more sensitive to their environment than 4f ones. Because of this, 3d impurities are better probes than rare earths to study the change on the optical

† To whom correspondence should be addressed. E-mail address: cases@posta.unizar.es.

0953-8984/98/419343+16$19.50

properties with the chlorine or bromine content. A brief previous study in an Ni^{2+}-doped fluorochlorozirconate glass [9], confirmed by x-ray absorption spectroscopy [10], indicates that chlorine ions are placed as Ni^{2+} first neighbours. In a recent paper we have reported on the optical properties of Cr^{3+} ions in fluorochloro- and fluorobromozirconate glasses [11]. The results have been interpreted in terms of the progressive substitution of the fluorine ions in the first coordination shell of Cr^{3+} by chlorines or bromines when the concentration of the latter in the glasses increases. Up to five different Cr^{3+} environments have been identified and assigned to: 6 F^-, 5 F^- and 1 Cl^- or 1 Br^-, 3 F^- and 3 Cl^- or 3 Br^-, 1 F^- and 5 Cl^- or 5 Br^- and 6 Cl^- or 6 Br^-. It was also found that a substitution of about 5% of the fluorine ions is enough to have almost all the Cr^{3+} ions hexacoordinated to chlorine or bromine ions [11].

The optical properties of Mn^{2+} in fluorozirconate glasses have been studied by different authors, and the results interpreted using the Tanabe–Sugano diagrams for an octahedral symmetry field [12–14]. The purpose of the present work is to use optical spectroscopy techniques (excitation, emission and decay measurements) to study the different environments of Mn^{2+} which are formed in fluorozirconate glasses when fluorines are partly substituted by chlorines or bromines.

2. Experimental details

2.1. Synthesis

Multicomponent Mn^{2+}-doped fluorozirconate, fluorochloro- and fluorobromozirconate glasses were prepared. The manganese-doped fluorozirconate glass with a starting composition (in mol%) of 52 ZrF_4, 20 BaF_2, 19.5 LiF, 4.5 LaF_3, 2.5 AlF_3 and 1.5 MnF_2 was prepared by standard methods [15]. Mixed halide glasses were prepared using NaF instead of LiF and appropriate quantities of BaX_2 and/or NaX (X = Cl or Br) instead of the corresponding amount of BaF_2 and/or NaF, and using a method of three stages, developed by Buñuel [16], following the method described in [3]. The starting compositions were 52 ZrF_4, $(20-x)$ BaF_2, x BaX_2, $(21-y-c)$ NaF, y NaX, 4.5 LaF_3, 2.5 AlF_3 and c MnF_2. The x, y and c values as well as the label of the samples used in this work are given in table 1. In this way, the starting concentration of chlorine or bromine (%X) with respect to the total halide content is $100(2x + y)/(290 + 2c)$. The samples are 2 mm thick and 2 cm diameter round pieces, and they are colourless except the most concentrated ones in chlorine or bromine which are slightly yellow. In the ZBr5 sample some white precipitates have been observed.

The actual composition of the samples was obtained by elemental microanalysis with an electron probe using a eXL Link Analytical x-ray microanalysis system in a JEOL JSM 6400 SEM (scanning electron microscope). For the x-ray detection an Si(Li) diode with a Be window was used. The electron energy was 20 keV and the measurements were performed with a probe current of 0.3 nA. The results obtained for chlorine and bromine content are summarized in table 1.

No glassy samples were obtained with an actual chlorine or bromine concentration larger than 7.8 or 7.2 respectively (taking into account the hardly vitreous aspect of the sample with 9.3% of bromine ions). On the other hand, these highest concentrations are almost the same as those that were introduced in this kind of glass doped with Er^{3+} [5–7] or Cr^{3+} [11].

Table 1. Nominal and measured content of substitute halide ions of the samples analysed by electron probe.

	BaX_2	NaX	MnF_2	% X	
Sample	*x*	*y*	*c*	Nominal	Measured
ZF	—	—	1.5	0.0	0.0
ZCl1	0.0	4.0	1.0	1.4	1.2
ZCl2	0.0	8.0	1.0	2.7	2.5
ZCl3	1.5	9.0	1.0	4.1	3.7
ZCl4	4.5	9.0	1.0	6.2	5.5
ZCl5	7.5	9.0	1.0	8.2	7.8
ZBr1	0.0	4.0	1.0	1.4	0.6
ZBr2	0.0	8.0	0.5	2.8	2.5
ZBr3	2.0	8.0	0.25	4.1	3.7
ZBr4	3.5	11.0	0.2	6.2	7.2
ZBr5	7.5	9.0	1.0	8.2	9.3

2.2. Optical measurements

Luminescence measurements were obtained by exciting the samples with either a 1000 W Oriel 66187 tungsten lamp followed by a double 0.5 m Spex 1680B monochromator or with a EG&G PAR Dyescan 2100 pulsed tunable dye laser (pulse duration of 1 ns and a spectral linewidth (FWHM) about 3 cm^{-1}). Fluorescence was detected through a 0.5 m Jarrell–Ash monochromator with a Hamamatsu R-928 photomultiplier tube for the spectral range between 200 and 800 nm. Lifetime measurements were carried out using a Tektronix 2430 digital storage oscilloscope triggered by the laser. The measurements at 10 K were taken in a CTI Cryogenics cooler. All the measurements have been corrected from the system response.

3. Experimental results

3.1. Excitation and steady state luminescence spectra

As we will show later, the luminescence spectrum of Mn^{2+} in our glasses is a broad band in the visible spectral range due to the superposition of the emissions of Mn^{2+} ions in different environments. To investigate these environments the excitation spectra detecting at different frequencies within the emission band have been measured at 10 K and room temperature (RT). Figure 1 shows the excitation spectra, taken at 10 K and detected at the energies given in the figure caption, of the ZF, ZBLAN:Cl:Mn^{2+} (figure 1(a)) and ZBLAN:Br:Mn^{2+} glasses (figure 1(b)). The chlorine or bromine concentration increases from the bottom to the top of the corresponding figure. The excitation spectrum of the ZF sample is well known as due to Mn^{2+} ions octahedrally coordinated with fluorines [12, 13]. The optical bands can be assigned using the corresponding Tanabe–Sugano (TS) diagram given in figure 2. The lowest energy band at about 20 000 cm^{-1} is assigned to the $^6A_{1g}(S) \rightarrow {}^4T_{1g}(G)$ transition. The sharp peak at about 25 000 cm^{-1} is assigned to the transition from the ground state to the $^4E_g(G)$, $^4A_{1g}(G)$ levels which are degenerated in our case although this degeneration can be broken by distortions and also by covalency and configurational interaction effects [17, 18]. The weak shoulder in the low energy tail of this peak is assigned to the $^6A_{1g}(S) \rightarrow {}^4T_{2g}(G)$ transition and finally, the broad band in

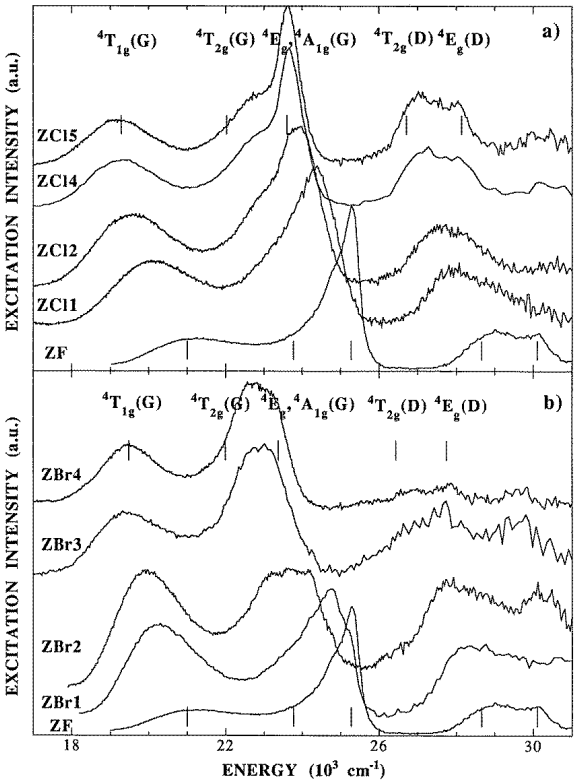

Figure 1. Excitation spectra of Mn^{2+} measured at 10 K and detected from bottom to top at: (a) 18 180, 16 130, 15 750, 15 620 and 15 380 cm^{-1} in the chloride and (b) 18 180, 17 540, 17 090, 16 000 and 15 870 cm^{-1} in the bromide samples. Ticks show calculated energy positions (see section 4.2).

the 28 000–31 000 cm^{-1} is assigned to two transitions: the lowest energy one is from the ground state to the $^4T_{2g}(D)$ level and the other one, to the $^4E_g(D)$ level. The transitions to spin doublets are not detected due to their very low oscillator strengths. We want to point out that, according with the TS diagram, all these transitions but the $^6A_{1g}(S) \rightarrow {}^4E_g(G)$, $^4A_{1g}(G)$ and the $^6A_{1g}(S) \rightarrow {}^4E_g(D)$ ones depend on the crystal field parameter Dq.

The spectra of the chloride and bromide samples show similar bands, allowing us to make the same assignments. The positions and the assignments of the excitation bands in the different samples are summarized in table 2.

A shift to the red is observed when the chlorine or bromine concentration increases. The shift of the band assigned to the $^6A_{1g}(S) \rightarrow {}^4T_{1g}(G)$ transition is slightly larger in the chloride than in the bromide samples. However, the opposite happens for the bands assigned to the $^6A_{1g}(S) \rightarrow {}^4E_g(G)$, $^4A_{1g}(G)$ and $^6A_{1g}(S) \rightarrow {}^4T_{2g}(D)$, $^4E_g(D)$ transitions. The main band in the ZF sample is the one assigned to the $^6A_{1g}(S) \rightarrow {}^4E_g$, $^4A_{1g}(G)$ transition. When the chlorine (or bromine) concentration increases this band broadens more than the others and its relative height decreases. The broadening and relative decrease reach a maximum for the samples with an intermediate concentration of chlorine or bromine ions.

RT measurements (not shown here) give similar results to those described above but the excitation bands are slightly shifted to higher energy and broadened with respect to low

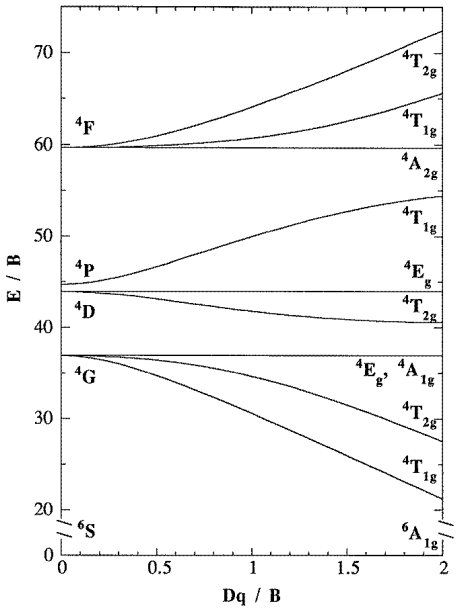

Figure 2. Tanabe–Sugano diagram of Mn^{2+} in O_h symmetry for a ratio $C/B = 5.38$ and $B = 650$ cm^{-1}.

Table 2. Maximum position (cm^{-1}), of the excitation bands of the transitions from the ground to the indicated levels for the chloride and bromide samples.

Sample	$^4T_{1g}$(G)	^4E_g, $^4A_{1g}$(G)	$^4T_{2g}$(D)	^4E_g(D)
ZF	21 050	25 300	29 000	30 230
ZCl1	20 000	24 300	27 800	—
ZCl2	19 600	24 000	27 500	—
ZCl4	19 200	23 600	27 000	28 160
ZCl5	19 200	23 600	27 000	28 150
ZBr1	20 200	24 750	28 050	—
ZBr2	19 850	23 750	27 650	—
ZBr3	19 350	23 100	26 900	27 850
ZBr4	19 400	23 100	26 900	27 850

temperature measurements.

Steady state emission spectra were measured at 10 K and RT in the fluorozirconate sample and in the chloride and bromide glasses, exciting the samples in several positions of their excitation spectra. Figure 3 shows the emission, measured at 10 K and excited at the maximum of the $^6A_{1g}(S) \rightarrow {}^4E_g(G)$, $^4A_{1g}(G)$ and $^6A_{1g}(S) \rightarrow {}^4T_{1g}(G)$ excitation bands for the chloride (figure 3(a)) samples and the bromide (figure 3(b)) ones respectively. The chlorine or bromine concentration increases from the bottom to the top of the corresponding figure. The only detected emission band corresponds to the $^4T_{1g}(G) \rightarrow {}^6A_{1g}(S)$ transition. In figure 3(b) the dashed line spectrum is obtained by exciting the ZBr5 sample at 18 300 cm^{-1}, and it corresponds to the Mn^{2+} ion emission in $MnBr_2$ crystals, which are present in some of our samples (see below). This emission disappears at 50 K. Figure 4

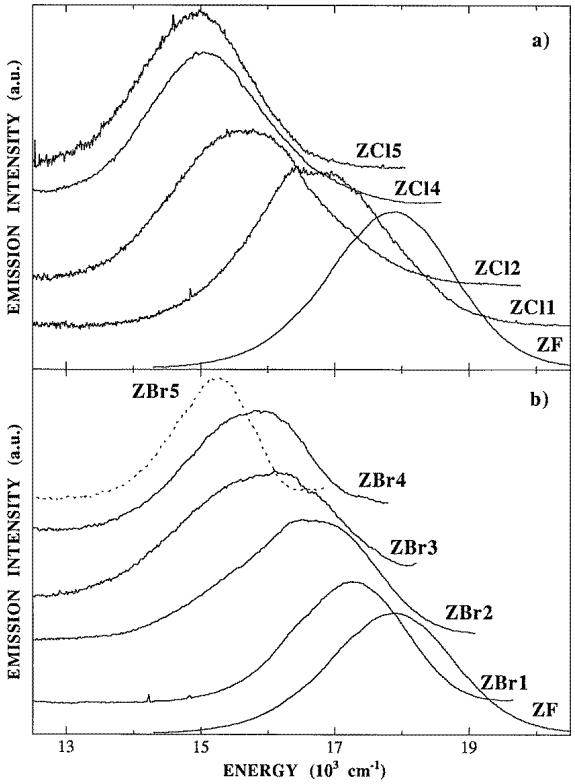

Figure 3. Steady state luminescence spectra of Mn^{2+} measured at 10 K and excited from bottom to top at: (a) 25 250, 24 250, 23 800, 23 600 and 23 500 cm^{-1} in the chloride and (b) 25 250, 20 300, 20 000, 19 400, 19 300 and 18 300 cm^{-1} in the bromide samples.

shows the evolution of the emission band maximum (figure 4(a)) and the full width at half maximum (FWHM) (figure 4(b)) with the chlorine or bromine concentration. A shift to lower energy, bigger for the chloride samples, is detected when the chlorine or bromine concentration increases. On the other hand a broadening with the chlorine or bromine content is observed which reaches a maximum value for the intermediate concentration samples; the most concentrated samples in chlorine or bromine present an emission band narrower than that in the fluorozirconate sample.

The spectra taken at RT (not given here) are similar to those measured at 10 K but the bands are broader and slightly shifted to higher energy. No relevant differences in the intensity of the emission bands were observed between 10 K and RT measurements.

Finally, some emission measurements, not shown here, were carried out exciting the samples at several positions along the $^6A_{1g}(S) \rightarrow {}^4T_{1g}(G)$ excitation band; these measurements present the same behaviour with the excitation energy as the one described above with the increase in chlorine or bromine content. The emission bands slightly shifts to the red as the excitation does.

The structural disorder in glasses is responsible for the broadening of the excitation and emission bands with respect to those in crystals. The dependence of the transition energies on the crystal field parameters can be useful to study the changes in the Mn^{2+} environment when the chlorine or bromine concentration increases. In order to do that detailed excitation

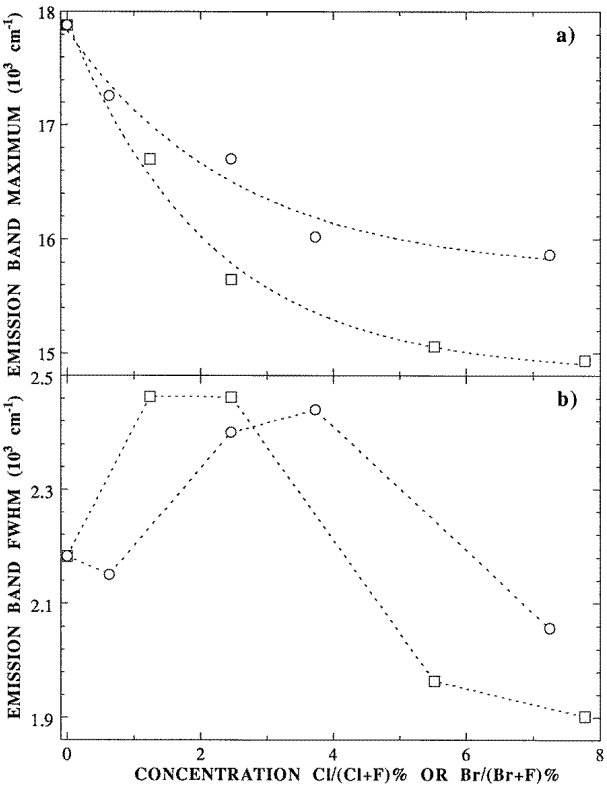

Figure 4. Evolution of the Mn^{2+} luminescence band maximum (a) and FWHM (full width at half maximum) (b) with the chlorine (squares) and bromine (circles) concentration. The lines are only a guide to the eye.

spectrum measurements have been performed in each sample detecting at different energies within the emission band. These excitation spectra, measured at 10 K, are given in figures 5 and 6 for the fluorozirconate and fluorochloride samples and in figures 7 and 8 for the fluorobromide ones. We want to point out that the results obtained with ZCl4 and ZCl5 are the same. Because of this most of our measurements have been performed in ZCl4. To obtain a clearer view, the different spectra have been vertically displaced. It can be seen that besides the red shift of the excitation bands with the chlorine or bromine content (already shown in figure 1), there is a shift to the red in each sample when the detection energy moves toward lower energies. Concerning the dependence of the $^6A_{1g}(S) \rightarrow {}^4E_g(G)$, $^4A_{1g}(G)$ transition band on the detection energy, the red shift is smaller for the most concentrated samples in fluorine, chlorine and bromine (ZF, ZCl4 and ZBr4) than for the samples of intermediate concentration. On the other hand, it can be observed in figures 5 and 6 that the spectrum detected in the high energy region of the ZCl1 sample is similar to those of the ZF sample; the measurement made in the high energy region of the ZCl2 sample is close to that detected at 16 130 cm^{-1} in ZCl1 and the spectrum detected in the high energy region of the ZCl4 sample is in between those detected at 15 750 and 17 860 cm^{-1} of the emission band in ZCl2. For the bromide samples, figures 7 and 8, the behaviour is similar: in this case the excitation spectrum detected in the high energy region in a sample is almost the same as that detected in the low energy region in the sample with the next lower bromine

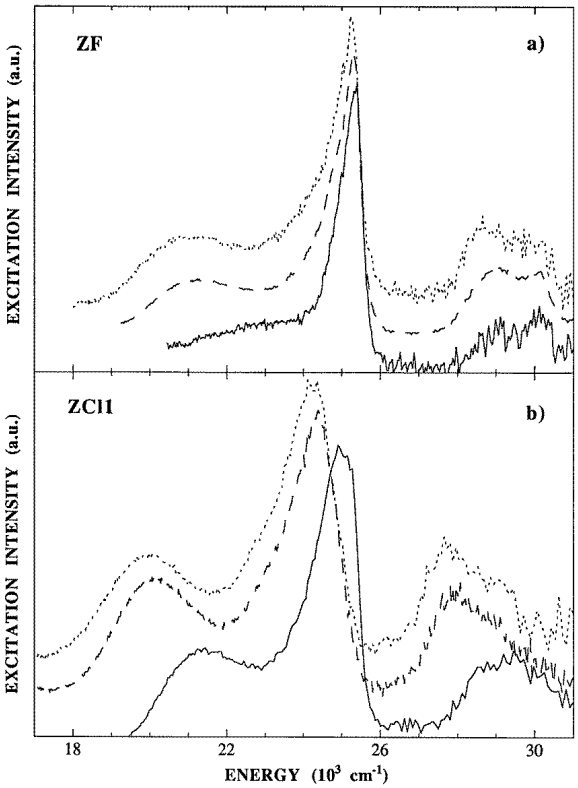

Figure 5. Excitation spectra of Mn^{2+} measured at 10 K and detected from bottom to top at: (a) 19 610, 18 180 and 16 530 cm^{-1} in ZF and (b) 18 690, 16 130 and 15 040 cm^{-1} in ZCl1 samples.

concentration. Narrow peaks at about 25 300, 23 600 and 23 100 cm^{-1} corresponding to the $^6A_{1g}(S) \rightarrow {}^4E_g(G)$, $^4A_{1g}(G)$ transition have been found in the most concentrated samples in fluorine (ZF), chlorine (ZCl4) and bromine (ZBr4) ions respectively. In the samples of intermediate concentration, the width and shape of the band, which are likely due to the coexistence of different environments for the Mn^{2+} ions, make it difficult to give accurate values for the position of the $^6A_{1g}(S) \rightarrow {}^4E_g(G)$, $^4A_{1g}(G)$ excitation band.

In the ZBr5 sample, with an almost polycrystalline aspect, the excitation spectrum measured at RT is similar to that in the ZBr4 one (these RT spectra are not shown). At 10 K (figure 8(b)), some new narrow bands appear that coincide with the excitation spectrum of Mn^{2+} ions in $MnBr_2$ crystal, where Pollini *et al* [19] showed that the Mn^{2+} ion is placed in octahedral symmetry with a very small trigonal distortion. At RT the emission of Mn^{2+} ions in these crystals is quenched. The narrow features of figure 8(b) slightly also appear for very low detection energies at 10 K in the ZBr4 and ZBr3 samples, indicating a very weak presence of $MnBr_2$ crystals in these samples.

3.2. Time dependent luminescence measurements

Luminescence decays were carried out at 10 K and RT in the fluorozirconate sample and at 10 K in the chloride and bromide ones. They have been excited at the maximum of

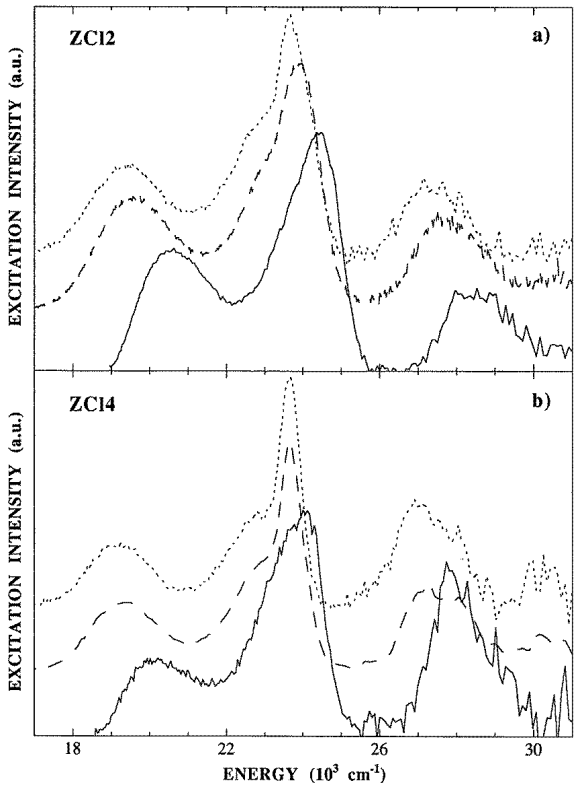

Figure 6. Excitation spectra of Mn^{2+} measured at 10 K and detected from bottom to top at: (a) 17 860, 15 750 and 14 080 cm^{-1} in ZCl2 and (b) 17 240, 15 620 and 13 790 cm^{-1} in ZCl4 samples.

the band corresponding to the $^6A_{1g}(S) \rightarrow {}^4T_{1g}(G)$ transition, and the luminescence light has been detected at the maximum and in the high and low energy tails of the emission band. The luminescence decays of fluorochloro- and fluorobromozirconate samples are shown in figures 9 and 10 respectively. The decays are not exponential and are faster for the bromide samples than for the fluorozirconate or chloride ones. There is a chlorine and bromine content dependence of the decays as a function of the detection energy. In the fluorozirconate sample the decay is faster when the detection energy moves to the blue; this is the same behaviour shown by RT measurements (not presented here), which are slightly faster than the 10 K ones. In the chloride samples the decay is faster when the detection energy moves to the low energy tail of the emission band. The differences among the decays are observed in the first 30 ms of each one. After this time the decays become almost exponential and similar in all the cases. In the bromide samples (figure 10), the decays are faster when the detection energy moves to the red for the sample with the smaller bromine content; there is almost no dependence on the detection energy in the sample of intermediate concentration of bromine but the decays are faster when the detection energy moves to the blue in the two most concentrated samples. In all the cases no dependence of the luminescence decays on the excitation energy was found.

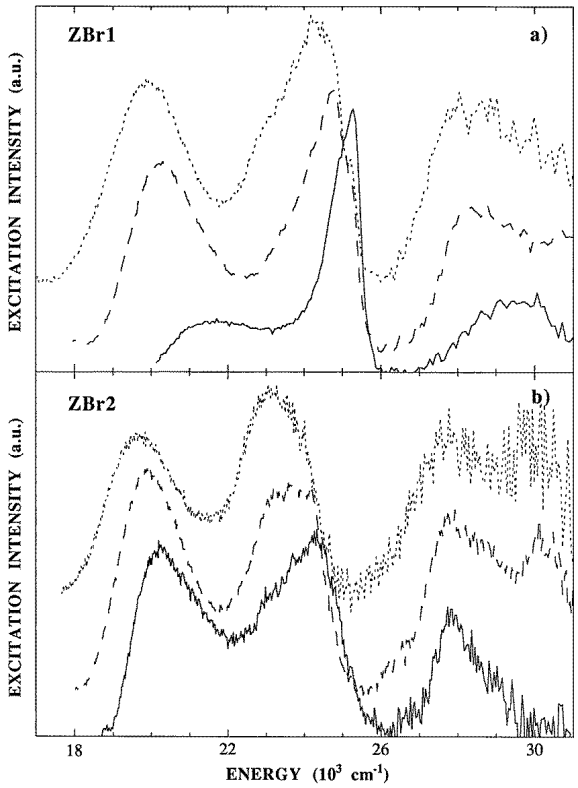

Figure 7. Excitation spectra of Mn^{2+} measured at 10 K and detected from bottom to top at: (a) 19 230, 17 540 and 15 380 cm^{-1} in ZBr1 and (b) 17 860, 17 090 and 16 390 cm^{-1} in ZBr2 samples.

4. Discussion

4.1. The Mn^{2+} ion environment

In the fluorozirconate sample the site distribution associated with the glass structure is responsible for the broadening of the excitation bands and for the red shift of the $^6A_{1g}(S) \rightarrow {}^4T_{1g}(G)$ excitation band when the detection energy moves to the red (figure 5(a)). As this transition depends on the crystal field and Racah parameters (Dq, B and C), we could think that there is a distribution of those parameters; but the narrowness of the band associated with the $^6A_{1g}(S) \rightarrow {}^4E_g(G)$, $^4A_{1g}(G)$ transitions (that only depend on the Racah parameters) and the fact that this band does not shift with the detection energy indicate that it is the crystal field parameter which is mainly distributed.

In the most concentrated samples in chlorine (ZCl4) or bromine (ZBr4), the position of the excitation bands to the ^4E_g, $^4A_{1g}(G)$ and $^4E_g(D)$ levels (figures 6(b) and 8(a)) which do not depend on Dq are close to those obtained for the same excitation bands of Mn^{2+} ions in the $MnCl_2$ and $MnBr_2$ crystals shown in [19]. This fact strongly suggests the same values for the B and C Racah parameters and so the same nature and number of the 3d ion ligands in our glassy samples and in the corresponding crystals. However, in the $MnCl_2$ and $MnBr_2$ crystals the lowest energy transitions ($^6A_{1g}(S) \rightarrow {}^4T_{1g}(G)$ and

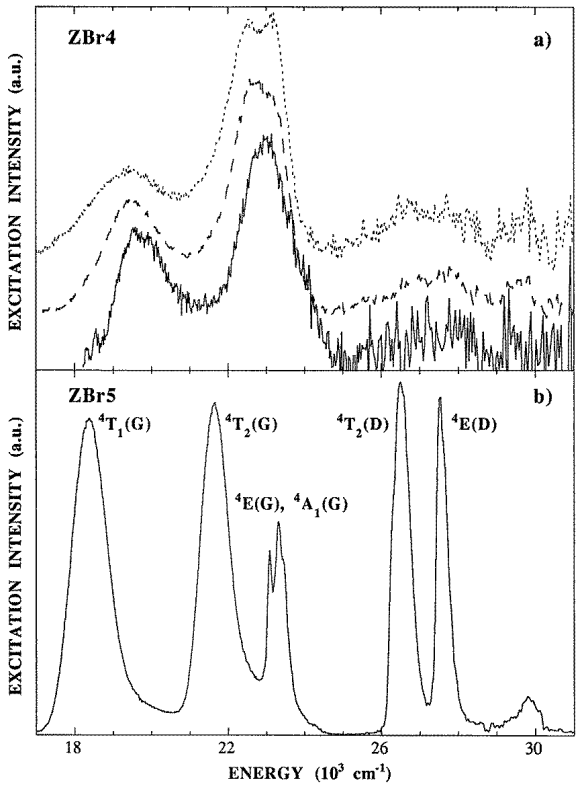

Figure 8. Excitation spectra of Mn^{2+} measured at 10 K and detected from bottom to top at: (a) 16 950, 15 870 and 14 920 cm^{-1} in ZBr4 and (b) 14 920 cm^{-1} in ZBr5 samples.

$^6A_{1g}(S) \rightarrow {}^4T_{2g}(G)$) which depend on *Dq* are red shifted from their positions in the ZCl4 and ZBr4 samples respectively. This indicates a larger *Dq* parameter and so a smaller 3d ion–ligand distance in crystals than in glasses. Moreover, we were not able to obtain samples with $^6A_{1g}(S) \rightarrow {}^4T_{1g}(G)$ excitation bands farther in the red. From all this we propose that the ZCl4 and ZBr4 excitation spectra detected in the low energy side of their emission bands are due to manganese ions octahedrally coordinated to six chlorine and six bromine ions respectively with a *Dq* distribution which is the responsible for the shift of the $^6A_{1g}(S) \rightarrow {}^4T_{1g}(G)$ excitation band with the detection energy (figures 6(b) and 8(a)).

In the samples with intermediate concentrations of chlorines or bromines the behaviour of the *Dq* independent bands ($^6A_{1g}(S) \rightarrow {}^4E_g$, $^4A_{1g}(G)$) with the chlorine or bromine content (figure 1) indicates that there is a composition dependence of the *B* and *C* parameters. This can be associated with the presence of chlorine or bromine ions in the Mn^{2+} neighbourhood. When the chlorine (bromine) content increases, different Mn^{2+} environments with an increasing number of Cl^- (Br^-) ions as manganese nearest neighbours will appear. We can have up to seven Mn^{2+} environments which range from Mn^{2+} ion coordinated to 6 F^- ions (ZF) to Mn^{2+} ion coordinated to 6 Cl^- or 6 Br^- ions (ZCl4 and ZBr4 respectively). The samples of intermediate concentrations of chlorine (bromine) ions will contain several mixed (F^-–Cl^- or F^-–Br^-) environments characterized by different *B* and *C* parameters. Each of these environments will have a distribution of sites (and

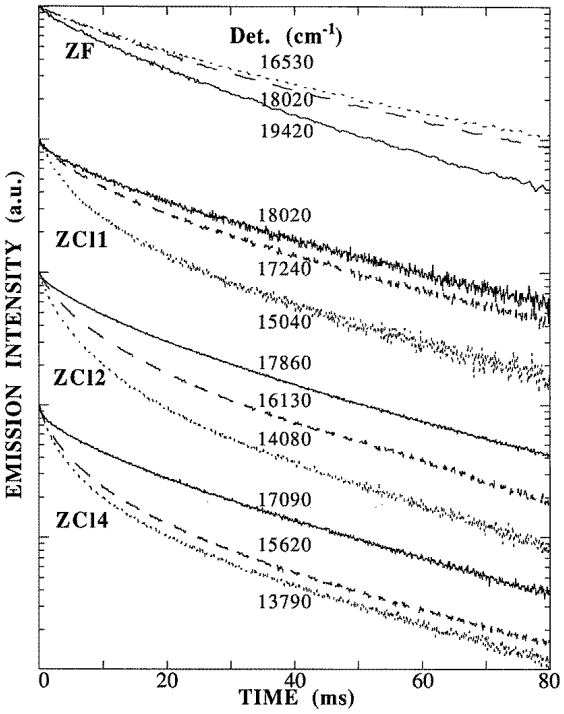

Figure 9. Mn^{2+} luminescence decays measured at 10 K and at the indicated detection (Det.) energies for the chloride samples. The excitation energies were: 21 000 (ZF), 20 000 (ZCl1), 19 650 (ZCl2) and 19 420 cm^{-1} (ZCl4).

consequently of Dq values) determined by the symmetry of the complex, the 3d ion–ligand distance etc. Environments with different B, C and Dq parameters give rise to different emission and excitation spectra. Thus we can understand that when we change the detection wavelength we are not looking at the same complexes and consequently we obtain different excitation spectra with the bands shifting from one to another.

On the other hand, the overlap of the shifted bands due to different environments produces a broadening that, in agreement with the experimental results, will be bigger for the samples with intermediate chlorine and bromine content in which the existence of different B, C and Dq parameters is larger. Besides, if these shifts are not very different in all the bands, it is easy to see that the relative broadening of the narrow ones, such as that associated with the $^6A_{1g}(S) \rightarrow {}^4E_g$, $^4A_{1g}(G)$ transition, is bigger than that of the broad bands, such as that due to the $^6A_{1g}(S) \rightarrow {}^4T_{1g}(G)$. This will also produce a larger relative decrease of the height of the narrow bands as compared with that of the broad ones, in agreement with the experimental results shown in figure 1.

Another consequence of the substitution of some of the fluorine ions of the Mn^{2+} complex by chlorines or bromines is the shift of the emission band along the chloride and bromide series (figure 4(a)) towards lower energy. The shift of this band that is associated with the $^4T_{1g}(G) \rightarrow {}^6A_{1g}(S)$ transition is due on one side to the increase of the ionic radius of the halogen ion (X^-) along the series $F^- \rightarrow Cl^- \rightarrow Br^-$. This increase produces in its turn an increase of the Mn^{2+}–X^- distance, and consequently, a decrease of the Dq value. In accordance with the Tanabe–Sugano diagram (figure 2) the decrease of Dq produces a blue

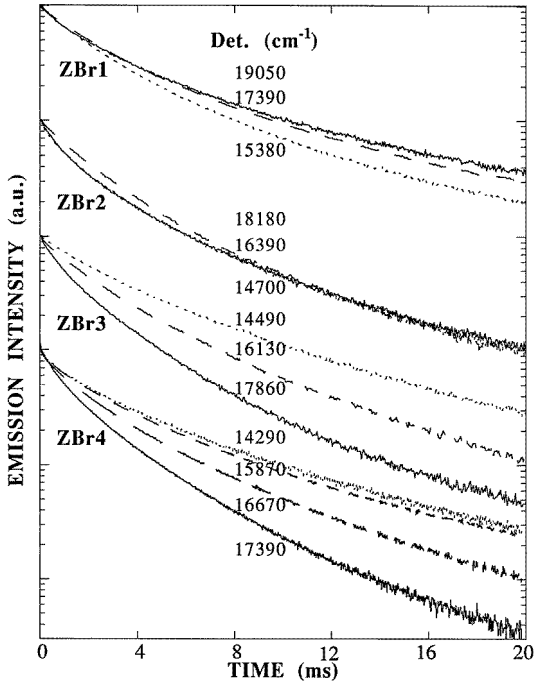

Figure 10. Mn^{2+} luminescence decays measured at 10 K and at the indicated detection (Det.) energies for the bromide samples. The excitation energies were: 20 100 (ZBr1), 19 800 (ZBr2), 19 530 (ZBr3) and 19 230 cm^{-1} (ZBr4).

shift of the emission band. On the other side, there is a decrease of the *B* parameter going from F^- to Cl^- and Br^- that produces a red shift of the emission band (see section 4.2). This red shift predominates over the blue one in all the samples but the difference between the two shifts is smaller in the bromide than in the chloride samples.

The increase of the FWHM of the $^4T_{1g}(G) \rightarrow {}^6A_{1g}(S)$ emission band in the samples with an intermediate concentration of chlorine or bromine ions (figure 4(b)) can be understood as a consequence of the coexistence of different mixed environments with a distorted octahedral symmetry in these samples. The presence of almost only a 6 Cl^- or 6 Br^- environment with octahedral symmetry in the most concentrated samples in substitute halide ions produces a new decrease of the emission band width. The narrowing of the emission band of the most chlorine or bromine concentrated samples with respect to the fluoride one may be due to the decrease of the energy of the local phonons involved in the emission process.

Concerning the identification of the different Mn^{2+} environments in our samples we have seen that samples ZCl4 (ZCl5) and ZBr4 mainly contain Mn^{2+} ions surrounded by six Cl^- or six Br^- respectively. Thus it can be concluded that a substitution of about 6% of the fluorines by chlorines or bromines seems to be enough to replace all the F^- ions around Mn^{2+} by Cl^- or Br^- ones. The detailed spectra of the $^6A_{1g}(S) \rightarrow {}^4E_g$, $^4A_{1g}(G)$ excitation bands of samples ZCl1, ZCl2, ZBr1 and ZBr2 (figures 5(b), 6(a), 7(a) and 7(b)) hardly show any narrow peaks that could be assigned to the presence of mixed environments namely one (5 F^- and 1 Cl^- or 1 Br^-), two (3 F^- and 3 Cl^- or 3 Br^-) and three (1 F^- and 5 Cl^- or 5 Br^-). Because of this we have not been able to unravel the presence of the different

Mn^{2+} environments in the samples with intermediate chlorine or bromine contents. This behaviour is different from that previously found for Cr^{3+} [11] where we took advantage of the sharpness of the spin-forbidden $^4A_{2g}(F) \rightarrow {}^2E_g(G)$, $^2T_{1g}(G)$ transitions to identify different Cr^{3+} complexes.

4.2. Crystal field calculations

Values of B, C and Dq parameters have been obtained by fitting the positions of the excitation bands calculated using the ligand field theory for a d^5 ion in octahedral symmetry to the experimental ones. This has been performed in the ZF, ZCl5 and ZBr4 samples whose excitation spectra are presented in figure 1. Because of the site distribution, the obtained parameters have to be considered as average values. The fitting was performed in the following way. The B and C parameters have been determined from the positions of the excitation bands corresponding to the transitions to the ^4E_g, $^4A_{1g}(G)$ and $^4E_g(D)$ levels; then, Dq is determined from the position of the excitation band to the first excited level $^4T_{1g}(G)$ and the B and C values previously obtained. Finally, the positions of the rest of the quartets were calculated using the Tanabe–Sugano matrix elements [20]. The position of the calculated levels has been plotted in vertical ticks and labelled with the corresponding level name in figure 1. The results obtained for the crystal field and Racah parameters are shown in table 3. The error in the estimation of the B and C values is about $\pm 4\%$ and that of Dq is $\pm 15\%$, but the important point is the trend of the results. A decrease of the three parameters going from the fluoride to either the chloride or the bromide sample is obtained. Besides B and Dq also decrease going from chlorides to bromides. In the samples with an intermediate concentration of chlorine or bromine ions, the coexistence of different Mn^{2+} environments, and probably an unknown local symmetry lower than octahedral, prevents us from performing a ligand field theory fitting.

Table 3. Crystal field and Racah parameters Dq, B and C (cm^{-1}) for the highest fluorine, chlorine and bromine content samples.

Sample	Dq	B	C
ZF	675	690	3675
ZCl5	665	650	3420
ZBr4	620	625	3425

The B and C values for the fluorozirconate sample are close to those found in this kind of glass [13] and also to those found in fluoride crystals [21–25]. Dq is also close to that in similar glasses [13] but smaller than in most of the fluoride crystals. Nevertheless in CdF_2:Mn^{2+} and CaF_2:Mn^{2+} [24], where it is well known that the 3d ion–ligand distance is large, Dq values similar to the one found in our glass have been found. In the same way, the B and C parameters for the most concentrated samples in chlorine and bromine ions are similar to those obtained in chloride and bromide crystals but the Dq values are smaller than in crystals [19, 26–29]. Some authors indicate that this effect is due to the fact that the 3d ion is placed in the Ba^{2+} ion position, which has a large ionic radius and a very strong modifier character in ZBLAN glasses [12].

The decrease of the Dq parameter with the substitute halide content is due to the bigger size of the chlorine and bromine ions, following the spectrochemical series, in such a way that the 3d ion–ligand distance cannot be the same than in the fluorozirconate sample. The decreases of the B and C parameters are due to the increase of the 3d ion–ligand

bonding covalence in the sense fluorine–chlorine–bromine following the nephaeleuxetic series. Finally the presence of Mn^{2+} coordinated to six chlorine or bromine ions in the most concentrated samples is also confirmed by the described behaviour of the Dq, B and C parameters indicating that for a substitute halide concentration higher than about 6%, almost all the fluorine ions have been replaced as Mn^{2+} first neighbours.

4.3. Time dependent luminescence properties

In order to explain the time dependent luminescence results (figures 9 and 10), we have tried to use the same processes (energy transfer and multiphonon non-radiative transitions) previously used to explain the decay results in Cr^{3+} doped fluorochloro- and fluorobromozirconate glasses [11]. As explained in [11] these two mechanisms produce opposite effects in the luminescence decay as a function of the detection wavelength. It is known that the sites that absorb (and emit) at lower energies have, in principle, larger multiphonon relaxation rates than those that absorb (and emit) at higher energies. On the other hand, the higher energy emitting sites can transfer their energy to those which emit (absorb) at lower energies while for the opposite process (transfer from lower to higher energies) it would be necessary to absorb also some phonons and this is a very unlikely process at 10 K. Taking all this into account the behaviour of the luminescence decay with the detection energy in ZF can be understood if the energy transfer processes are dominant with respect to the multiphonon ones because in this way the sites that emit at higher energy will decay faster than those emitting at lower energies in agreement with the experimental results.

In the chloride samples although the Mn^{2+} concentration (1%) is similar to that of the ZF sample and so we should think again in dominant energy transfer processes, the dependence on the detection energy does not allow us to use this explanation. Moreover, we have found that the decays as a function of the detection energy of a sample with the same chlorine content as ZCl2 but with 0.125% of Mn^{2+} present the same behaviour as those of the sample ZCl2. Since energy transfer is strongly dependent on the concentration of 3d ions we should conclude that those processes are not the dominant ones in fluorochloride samples. Although the non-radiative transitions to the ground state seem to be smaller in the Mn^{2+} than in the Cr^{3+} ion [11] due to the greater energy gap between the first excited and ground states, the use of that mechanism in the way described in [11] could account for the greater non-radiative transition probability for the sites which emit at lower energies. The most concentrated samples in bromine ions present the same behaviour with the detection energy as described in ZF, but much faster. Because the sites that emit at higher energies have shorter decays the energy transfer mechanism should be also dominating in those samples, although they have the smallest concentration in Mn^{2+} ions (table 1). In samples with low bromine content we should consider that multiphonon processes dominate and for intermediate bromine concentrations an increasing energy transfer contribution should be assumed. From all these results we have to conclude that the behaviour of the decays versus the detection energy is very complicated and it does not seem easy to explain it with the same mechanisms as used in the case of Cr^{3+} ions. A more detailed work as a function of temperature and Mn^{2+} concentration will be necessary to clarify this problem.

5. Conclusions

Some Mn^{2+} doped fluorozirconate and fluorochloro- and fluorobromozirconate glasses have been prepared following and improving some standard methods. The actual composition

of the samples has been determined by an electron probe microanalysis. The maximum concentration of chlorine or bromine ions that has been possible to introduce in the fluorozirconate composition is about 7%.

Optical excitation, steady state luminescence and time dependent luminescence measurements have been performed in the whole set of prepared samples in order to study the Mn^{2+} environment and its optical properties. A progressive substitution of the fluorine ions of the Mn^{2+} complex by chlorine or bromine ones takes place when the chlorine or bromine content increases in the glasses. It is remarkable that almost all the Mn^{2+} are hexacoordinated with chlorine or bromine ions for a concentration of the substitute halide ions higher than 6%, which indicates a preference of these ions to occupy those non-bridging positions close to the 3d ion.

Acknowledgments

Support for this work has been received from the DGICYT (Spain) under contract No PB94-0550 and from the local government (DGA) under contract No PCB0494. M A Buñuel thanks DGA and MEC for financial support.

References

[1] Almeida R M (ed) 1987 *Halide Glasses for Infrared Fiberoptics (NATO ASI Series E-123)* (Dordrecht: Nijhoff)
[2] France P W, Drexhage M G, Parker J M, Moore M W, Carter S F and Wright J V 1990 *Fluoride Glass Optical Fibers* (Glasgow: Blackie)
[3] Elyamani A, Poulain M, Saggese S J and Siegel G H Jr 1990 *J. Non-Cryst. Solids* **119** 187
[4] Inoue H, Soga K, Makishima A and Yasui I 1995 *Phys Chem. Glasses* **36** 1
[5] Takahashi M, Yamamoto R, Kanno R and Kawamoto Y 1995 *J. Phys.: Condens. Matter* **7** 4583
[6] Takahashi M, Kanno R, Kawamoto Y and Kadono K 1995 *J. Phys.: Condens. Matter* **7** 7797
[7] Kawamoto Y, Kanno R, Yokota R, Takahashi M, Tanabe S and Hirao K 1993 *J. Solid State Chem.* **103** 334
[8] Soga K, Uo M, Inoue H and Makishima A 1995 *J. Am. Ceram. Soc.* **78** 129
[9] Buñuel M A, Alcala R and Cases R 1995 *Radiat. Eff. Defects Solids* **135** 23
[10] Buñuel M A, Cases R, Garcia J, Proietti M G and Solera J A 1997 *J. Physique* IV **7** 1219
[11] Buñuel M A, Alcalá R and Cases R 1998 *J. Chem. Phys.* **109** 2294
[12] Feuerhelm L N, Sibley S M and Sibley W A 1984 *J. Solid. State Chem.* **54** 164
[13] Suzuki Y, Sibley W A, El Bayoumi O H, Roberts T M and Bendow B 1987 *Phys. Rev.* B **35** 4472
[14] Cases R, Buñuel M A, Alcala R and Orera V M 1993 *Proc. 12th Int. Conf. on Defects in Insulating Materials* ed O Kannert and J M Speath (Singapore: World Scientific) p 905
[15] Poulain M 1983 *J. Non-Cryst. Solids* **56** 1
[16] Buñuel M A 1997 *Doctoral Dissertation* University of Zaragoza
[17] Ghosh B and Mukherjee R K 1981 *Phys. Status Solidi* b **106** 699
[18] Sharma R R, Viccaro M H de A and Sundaram S 1981 *Phys. Rev.* B **23** 738
[19] Pollini I, Spinolo G and Benedek G 1980 *Phys. Rev.* B **22** 6369
[20] Tanabe Y and Sugano S 1954 *J. Phys. Soc. Japan* **9** 753
Tanabe Y and Sugano S 1954 *J. Phys. Soc. Japan* **9** 766
[21] Mehra A K and Venkateswarlu P 1967 *J. Chem. Phys.* **47** 2334
[22] Srivastava J P 1972 *J. Chem. Phys.* **37** 1587
[23] Alonso P J, Orera V M, Palacio F and Alcala R 1982 *Phys. Status Solidi* b **109** K81
[24] Alonso P J and Alcala R 1981 *J. Lumin.* **22** 321
[25] Rodriguez F and Moreno M 1986 *J. Chem. Phys.* **84** 692
[26] Talapatra D and Mukherjee R K 1989 *Phys. Status Solidi* b **155** 541
[27] Trutia A, Ghiordanescu V and Voda M 1975 *Phys. Status Solidi* b **70** K19
[28] Talapatra D, Ghosh B and Mukherjee R K 1991 *Nuovo Cimento* **13** 859
[29] Marco de Lucas C, Rodriguez F and Moreno M 1992 *Phys. Status Solidi* b **172** 719